Nonlinear Dyn (2019) 98:215–231
https://doi.org/10.1007/s11071-019-05184-2

ORIGINAL PAPER

Reliable and efficient processing of sensory information at body temperature by rodent cortical neurons

Xin Fu · Yuguo Yu

Received: 20 January 2019 / Accepted: 3 August 2019 / Published online: 15 August 2019
© Springer Nature B.V. 2019

Abstract Some pathological conditions, such as infections and febrile seizures, may cause temperature fluctuations in the brain. We ask here how these temperature fluctuations, particularly hypothermia and hyperthermia, affect the cortical information coding performance and response reliability of warm-blooded animals. We studied this issue by a combination of in vitro whole-cell patch clamp recordings from cortical pyramidal neurons and computational simulations of Hodgkin–Huxley cortical neuronal model at different temperatures. A significantly higher reliability of the neuronal response to repeated input signals was observed at physiological temperature ($\sim$ 35 °C) than that at a much lower temperature ($\sim$ 24 °C) or upon hyperthermia ($\sim$ 41 °C). In addition, the firing rate of excitatory neurons (i.e., pyramidal neurons) was increased gradually, while it decreased gradually for inhibitory neurons (e.g., PV interneurons) as the temperature increased from 25 to 40 °C. The opposite changes in the response activity level between pyramidal neurons and interneurons suggested a shift in the excitatory/inhibitory (E/I) balance in the local network circuit as a function of changing temperature. An analysis of the information coding efficiency suggested that the pyramidal neurons displayed the maximal response reliability with the highest coding efficiency and information transmission rate at body temperature, suggesting that the E/I balance observed at this temperature might be optimal for enhancing information coding in cortical neurons. In addition, we applied tetrodotoxin and 4-aminopyridine to partially block Na^+ and K^+ channels, respectively, and observed that a change in sodium or potassium conductance could also alter the neuronal response reliability of pyramidal neurons.

Keywords Pyramidal neuron · Hodgkin–Huxley model · Response reliability · Coding efficiency · Information transmission rate

1 Introduction

Intrinsic and external factors influencing the information processing capability of cortical neurons have been widely studied in the past few decades [1–6]. The factors inducing variations in the neuronal responses to repeated input signal are derived from a broad range of sources, such as channel noises, spontaneous synaptic activities and the mechanism regulating inhibitory circuits [7–9]. Evidences indicate that neuronal responses are typically nonlinear and could be affected by many external factors. For example, the background stochastic synaptic noise may enhance neuronal detection abil-

X. Fu
College of Biosciences, Fudan University, Shanghai 200433, China

Y. Yu (✉)
State Key Laboratory of Medical Neurobiology, School of Life Science and Human Phenome Institute, Institutes of Brain Science, Institute of Science and Technology for Brain-Inspired Intelligence, Fudan University, Shanghai 200433, China
e-mail: yuyuguo@fudan.edu.cn

ity to weak input signal via stochastic resonance mechanism [10–12]. In addition, the spike reliability of cortical neurons is also tuned by stimulus frequency [13,14]. It was reported that pyramidal neurons show high reliability for signals with relatively low-frequency components, while interneurons show high reliability to high-frequency input signals [13]. The response reliability of cortical neurons is reduced by optogenetic suppression of parvalbumin (PV)-expressing interneurons or the application of the $GABA_A$ receptor blocker gabazine [9,15]. It is also reported recently that a specific autaptic activity could regulate the firing dynamics and improve spike timing precision of fast-spiking interneurons [16,17]. Thus, the cortical information coding reliability could be affected by rich factors from both intrinsic properties (e.g., stochastic nature of ionic channels, morphological and physiological parameters of individual neuron) and external network environments (e.g., stochastic synaptic noise and inhibitory circuits).

In addition, it is noteworthy that the neuronal network plays a crucial role in cognitive functions and information processing [18]. The rhythmic behaviors of neuronal network oscillations may appear in different patterns, such as synchrony or chimera state. The chimera state is a peculiar type of dynamical phenomenon which is a coexistence of synchronous and asynchronous oscillations in network [19]. Although the chimera like anomalous synchronization resembles certain pathological brain disorder states like epileptic seizures and schizophrenia [19,20], some of the synchronous oscillations could enhance the reliability of communications. The neuronal information encoding capacities could be maximized by the optimal synchronous states in the network [21]. Network rhythmicity may protect the reliable information transmission for neuronal network in the noisy environment.

Due to the complex neuronal physiological properties and network rhythmicity across neurons, there are still more factors to be examined with regard to their influence on the neural information processing, e.g., temperature. The frequency and duration of rhythmic oscillations and spiking properties of individual neurons may be heavily affected by fluctuations of body temperature [22,23]. In vivo, the activation properties of neurons may be mainly dominated by the physiological conditions of the studied animals, and even small physiological fluctuation in body temperature is known to alter the neuronal processes and responses dramatically [24].

Under normal conditions, warm-blooded animals, e.g., birds, mammals and primates, generally have a warm body temperature of approximately 37 °C compared with ectothermic animals, whose body temperatures fluctuate with the environment [25]. The body temperature of endothermic animals is tightly regulated by hypothalamus [26,27], and temperature fluctuations potentially alter neuronal responses and influence brain functions [24,28]. Thus, a constant warm body temperature is an important factor influencing the survival of those warm-blooded animals. However, the mechanisms by which temperature fluctuations affect the cortical information coding and response reliability have been rarely studied in the past few decades.

Some pathological conditions, such as infections and febrile seizures, cause temperature fluctuations in the brain [29]. Much lower (< 20 °C) or higher (> 40 °C) temperature may induce serious alterations in the functions of the brain. In patients with certain clinical conditions, numerous investigators observed that a certain reduction in temperature protects the brain from ischemic injury [30]. Moderate hypothermia (30–31 °C) results in burst suppression in patients with the generalized status epilepticus [31]. Hypo-metabolism may trigger cognitive decline and induce neurodegeneration [32]. Additionally, hyperthermia up to 41 °C causes hyperexcitability of pyramidal neurons in the hippocampus and prefrontal cortex by directly altering the intrinsic membrane properties [33,34]. A shift in the temperature from room temperature (RT) to physiological temperature (PT) switches the firing pattern of neocortical pyramidal neurons from burst spiking to regular firing [23]. Compared with RT, the efficiency of energy utilization for the generation of a single action potential (AP) in pyramidal neurons from the somatosensory cortex is substantially increased at PT [35]. The variations in body temperatures with environmental conditions may seriously limit the neuronal information coding accuracy, since the precise opening and closing of ion channels strongly depend on temperature. Temperature influences the dynamic characteristics of all ion channels as a global perturbation that dramatically changes the basic intrinsic membrane property and synaptic transmission [36]. At a warm body temperature, the synaptic connections show fewer apparent transmission failures, less trial-to-trial variability and a higher transmitter release probability than at RT [37–39]. Consequently, a warm body temperature improves the neuronal energy efficiency and reliability

of synaptic transmission. Although numerous studies have discussed the effects of temperature on neuronal properties and functions, the mechanisms by which temperature alters neuronal information processing, e.g., the response reliability and information coding, at the individual cortical neuron level remain elusive.

Here we carried out a set of experiments and computational simulations of neuronal model. We aimed to examine how the neuronal response reliability and coding efficiency could be altered by a change in temperature, and what factors were fundamental underlying temperature-dependent neural coding accuracy and reliability.

2 Materials and methods

2.1 Brain slice preparation

The conducts and procedures involving animal experiments were approved by the Animal Ethics Committee of Fudan University School of Life Sciences. Wild-type C57 mice (male or female, postnatal days 10–18) were used in this study. Under deep chloral hydrate anesthesia, a mouse was decapitated and the brain was quickly removed and placed in a 0–4 °C carbogen-bubbled (95% O_2 and 5% CO_2) ice-cold cutting solution (in mM): 92 *N*-methyl-D-glucamine (NMDG), 2.5 KCl, 10 $MgSO_4$, 0.5 $CaCl_2$, 1.2 NaH_2PO_4, 30 $NaHCO_3$, 20 HEPES, 25 D-glucose, 5 sodium-L-ascorbate, 2 mM thiourea and 3 mM Na-pyruvate (300–310 mOsm, pH 7.3–7.4, corrected with hydrochloric acid). The posterior 30% of the brain was resected with a coronal cut, and the remaining portion containing the prefrontal cortex was attached to the cutting stage of a vibratome (VT1000S, Leica). The tissue was sectioned into 300 μm coronal slices and incubated in artificial cerebrospinal fluid (ACSF) at 35 °C for 30 min. ACSF contained (in mM): 119 NaCl, 2.5 KCl, 1.25 NaH_2PO_4, 24 $NaHCO_3$, 2 $MgSO_4$, 2 $CaCl_2$, 12.5 D-glucose (300–310 mOsm, pH 7.3–7.4). Then, the slices were maintained at RT in a chamber for an additional 30 min before recordings.

2.2 Electrophysiological recordings

For whole-cell patch clamp recordings, a slice was transferred to recording chamber and bathed in oxygen-saturated ACSF flowing at a rate of 3–4 ml/min. Deep layer cortical neurons (layer V/VI) were targeted with an upright infrared differential interference contrast microscope (BX-51WI, Olympus) and a CCD camera (IR-1000E, DAGE-MTI). Recordings were performed with a Multiclamp 700B amplifier (Axon Instruments) and Micro1401 with Spike2 software (CED, Cambridge). Signals were low-pass filtered at 10 kHz and sampled at 25 kHz. The temperature was controlled with temperature controller (TC344C, Warner), and we used three temperature gradients in our study: RT (24 ± 2 °C), PT (35 ± 2 °C) and high temperature (HT, 41 ± 2 °C).

Whole-cell recordings were obtained with micropipettes with a 5–9 MΩ tip resistance filled with an intracellular solution containing (in mM) 130 K-gluconate, 7 KCl, 10 HEPES, 4 Mg-ATP, 0.3 Na-GTP, 10 Na-phosphocreatine and 0.2 EGTA (280–290 mOsm, pH 7.2–7.3, adjusted with KOH). Tight seals (> 1 GΩ) were formed before the membranes were ruptured with negative pressures or voltage zaps. ACSF was supplemented with 1 mM 4-aminopyridine (4-AP) or 10 nM tetrodotoxin (TTX) to partially block K^+ or Na^+ channels, respectively. The liquid junction potential was 15 mV, and it was not corrected in the reported data.

The injected repeated signals (duration was 1 s) were constructed by using Gaussian colored noise (the noise intensity was quantified by its standard deviation σ) filtered by low-pass filter with cutoff frequency of 500 Hz. The injected signals mimicked a mixture of synaptic potentials that were composed of excitatory and inhibitory synaptic inputs. One additional nonrepeated weak Gaussian colored noise with a noise intensity of approximately $0.4\,\sigma$ of the repeated signal was used to control the background spontaneous firing rate in most of the experiments. At each examined temperature, the repeated input signal was injected repeatedly to the recording neuron with a 1 s duration for 45 trials (a 3-s nonsignal period with only nonrepeated noise input between the repeated trials was implemented).

2.3 Hodgkin–Huxley-style cortical neuronal model

There were three ionic voltage-dependent currents in our Hodgkin–Huxley (HH) cortical neuronal model: fast Na^+, I_{Na}, fast K^+, I_K, and a leak current, I_L. The equations describing the voltage and time dependence

of the ionic currents were based upon previous publications [40,41]. The equations were as follows:

$$C\frac{\mathrm{d}V}{\mathrm{d}t} = I_{\mathrm{stim}} - g_{\mathrm{Na}}^{\max}\cdot m^3\cdot h\cdot(V-V_{\mathrm{Na}}) - g_{\mathrm{K}}^{\max}\cdot n\cdot(V-V_{\mathrm{K}}) - g_{\mathrm{L}}\cdot(V-V_{\mathrm{L}})$$

$$\tau_m\frac{\mathrm{d}m}{\mathrm{d}t} = -m+m_\infty,\ \tau_m = \frac{1}{\alpha_m+\beta_m},\quad m_\infty = \frac{\alpha_m}{\alpha_m+\beta_m}$$

$$\tau_h\frac{\mathrm{d}h}{\mathrm{d}t} = -h+h_\infty,\ \tau_h = \frac{1}{\alpha_h+\beta_h},\quad h_\infty = \frac{1}{1+e^{(V+60)/6.2}}$$

$$\tau_n\frac{\mathrm{d}n}{\mathrm{d}t} = -n+n_\infty,\ \tau_n = \frac{1}{\alpha_n+\beta_n},\quad n_\infty = \frac{\alpha_n}{\alpha_n+\beta_n}$$

$$\alpha_m(V) = \phi\cdot\frac{0.182\cdot(V+30)}{1-e^{-(V+30)/8}}$$

$$\beta_m(V) = -\phi\cdot\frac{0.124\cdot(V+30)}{1-e^{(V+30)/8}}$$

$$\alpha_h(V) = \phi\cdot\frac{0.028\cdot(V+45)}{1-e^{-(V+45)/6}}$$

$$\beta_h(V) = -\phi\cdot\frac{0.0091\cdot(V+70)}{1-e^{(V+70)/6}}$$

$$\alpha_n(V) = \phi\cdot\frac{0.01\cdot(V-30)}{1-e^{-(V-30)/9}}$$

$$\beta_n(V) = -\phi\cdot\frac{0.002\cdot(V-30)}{1-e^{(V-30)/9}}$$

$$\phi = Q_{10}^{(T-23)/10},$$

where Φ regulated the temperature dependence of the rate constants, with $Q_{10} = 2.3$. The parameters used in our cortical neuronal model were: membrane capacitance (C) = 0.75 μF/cm^2, $g_{\mathrm{Na}}^{\max}$ = 1500 pS/μm^2, $g_{\mathrm{K}}^{\max}$ = 60 pS/μm^2 and g_{l} = 0.33 pS/μm^2. The reversal potentials of leak, Na^+ and K^+ channels were $V_{\mathrm{L}} = -70$ mV, $V_{\mathrm{Na}} = 60$ mV and $V_{\mathrm{K}} = -90$ mV, respectively. The injected repeated signal was Gaussian colored noise (σ = 1 μA/cm^2) and was injected repeatedly with a 0.5 s duration for 100 trials, and one additional nonrepeated weak Gaussian colored noise with a noise intensity of approximately 0.1 σ of the repeated signal was used to control the background spontaneous firing rate.

2.4 Data analysis

We calculated cross-covariations between all pairwise combinations of the repeated trials to estimate the response reliability. The recorded spike trains were transformed into 0 and 1 binary vectors ('1' represented the firing of an AP and '0' represented non-AP responses), and cross-covariance analyses between pairs of combinations of all the trials were performed. The value of cross-covariance at zero lag was used to quantify the response reliability. A small value near 0 suggested that the repeatable neuronal responses did not occur across the trials, and a large value near 1 indicated the highest repeatable neuronal response.

We calculated the information entropy rate and coding efficiency using direct entropy calculation methods to measure the efficiency and rate of information transmission [42]. First, we calculated the total response entropy rate (H_{total}) of the spike train with a long time period (around 70–100 s for experiment and 150 s used for HH cortical neuronal model), which was used to represent the maximal information capacity of the studied neuron that was excited by a nonrepeated random Gaussian colored noise (σ = 500 pA for experiment and σ = 1 μA/cm^2 for HH cortical neuronal model). The spike train was translated into a train sequence of a 1 (representing one spike in a time bin $\Delta\tau$) and 0 (no spikes in the bin $\Delta\tau$) binary vector. For any given time window T_{s}, $T_{\mathrm{s}}/\Delta\tau$ letters were presented, which constituted a 'word.' Next, we varied the length of the time window T_{s} and calculated the normalized probability of different words p_{i} in the whole train sequence. Then, the naive estimate of the entropy S_{naive} for the spike train sequence was calculated using the following equations:

$$S_{\mathrm{naive}}(T_{\mathrm{s}},\Delta\tau,\mathrm{size}) = -\sum_i p_i\log_2 p_i$$

$$H_{\mathrm{total}} = -\lim_{T_{\mathrm{s}},\mathrm{size}\to\infty} S_{\mathrm{naive}}(T_{\mathrm{s}},\Delta\tau,\mathrm{size})/T_{\mathrm{s}},$$

where H_{total} is the total response entropy rate.

The noise entropy rate (H_{noise}) quantified the response variability following repeated exposure to the same time-varying noise stimulus. For a given time t relative to the stimulus, we calculated the possibilities of the occurrence of $p_i(t)$ for each word i that begins at t. Then, the naive estimate of the local noise entropy

in the time window (t to $t + T_s$) was calculated as follows:

$$N_{\text{naive}}^{\text{local}}(t, T_s, \Delta\tau, \text{size}) = -\sum_i p_i(t) \log_2 p_i(t).$$

Next, we calculated the average noise entropy over t

$$N_{\text{naive}}(T_s, \Delta\tau, \text{size}) = \left\langle N_{\text{naive}}^{\text{local}}(t, T_s, \Delta\tau, \text{size}) \right\rangle_t .$$

Subsequently, we estimated the noise entropy rate by extrapolating to a large data set size and for the large T_s

$$H_{\text{noise}} = -\lim_{T_s, \text{size}\to\infty} N_{\text{naive}}(T_s, \Delta\tau, \text{size})\,/T_s.$$

Mutual information (MI) reflected the information rate in the response that directly correlated with the stimulus. MI was described as

$$\text{MI} = H_{\text{total}} - H_{\text{noise}}.$$

The information transmission rate was measured as MI/⟨mean firing rate⟩, which quantified how much information was carried by an individual action potential. The coding efficiency was defined as $\text{MI}/H_{\text{total}}$, which quantified the fraction of neuronal activity that encoded the input signal.

Data were processed using GraphPad Prism 5.0 and SigmaPlot 10.1 software. Data were reported as the means ± s.e.m., and a paired t test was used for the analysis ($^*p < 0.05$, $^{**}p < 0.01$ and $^{***}p < 0.001$).

3 Results

3.1 The maximal neuronal response reliability was observed at PT

We first studied the neuronal response reliability to repeated input signals at different temperatures to investigate the extent to which temperature fluctuations influenced the information processing accuracy of cortex pyramidal neurons.

We performed whole-cell patch clamp recordings of layer V/VI pyramidal neurons in the mouse prefrontal cortex at RT, PT and HT. The membrane potential depolarized from -62.89 ± 1.03 mV at RT to -48.21 ± 2.01 mV at HT ($p < 0.001$; paired t test; $n = 15$; Fig. 1c and red line in Fig. 1a) as the temperature increased. The firing rate increased with the increase in temperature (although the differences among different temperatures were not significant, $p > 0.05$; paired t test; $n = 15$) as shown in Fig. 1c. Each vertical line in the raster plots of the firing timing represented the firing of an AP. According to the raster plots and peristimulus time histograms (PSTHs) shown in Fig. 1a, the neurons displayed more reproducible responses to repeated noise signals with σ of 500 pA at PT than at RT and HT. Based on the results of the statistical analyses, the reliability of neuronal spiking was 0.77 ± 0.04 at PT, a value that was significantly greater than the values observed at RT (0.70 ± 0.05; $p < 0.001$; paired t test) and HT (0.75 ± 0.04; $p < 0.05$; paired t test) ($n = 15$; Fig. 1b). The same experiments were conducted at different noise intensities ($\sigma = 357$ and 625 pA), and the maximal neuronal response reliability was observed at PT (0.76 ± 0.05 at 375 pA, $p < 0.001$ for the comparison between RT and PT and $p < 0.01$ for the comparison between PT and HT, paired t test, $n = 11$; 0.79 ± 0.05 at 625 pA, $p < 0.001$ for the comparison between RT and PT and $p < 0.05$ for the comparison between PT and HT, paired t test, $n = 12$) in all the tested experiments (Fig. 1d). Compared with PT, the percentages of the decreased reliability were 10.1% at RT and 8.29% at HT for 375 pA ($n = 11$), 11.35% at RT and 2.92% at HT for 500 pA ($n = 15$), and 10.6% at RT and 5.48% at HT for 625 pA ($n = 12$). The decreased reliabilities recorded at RT and HT did not depend on the stimulus intensities. Thus, the neuronal response reliability exhibited a global maximum when the temperature was approximately PT.

3.2 The relationship between RMP, stimulus intensity and response reliability

Based on the data, a warm temperature resulted in a depolarized RMP ($p < 0.01$ for the comparison between RT and PT and $p < 0.001$ for the comparison between PT and HT; paired t test) and an increased firing rate (no significant differences between RT, PT and HT, $p > 0.05$) of pyramidal neurons (Fig. 1c). Multiple factors may contribute to the maximal response reliability observed for cortical neurons at PT than at other temperatures. The factors included changes in the membrane potential and firing rate. We next performed the experiments described below to examine the dependence of the response reliability on the stimulus intensity and RMP level.

First, we studied the effects of different stimulus intensities on spiking reliability. Noise intensities

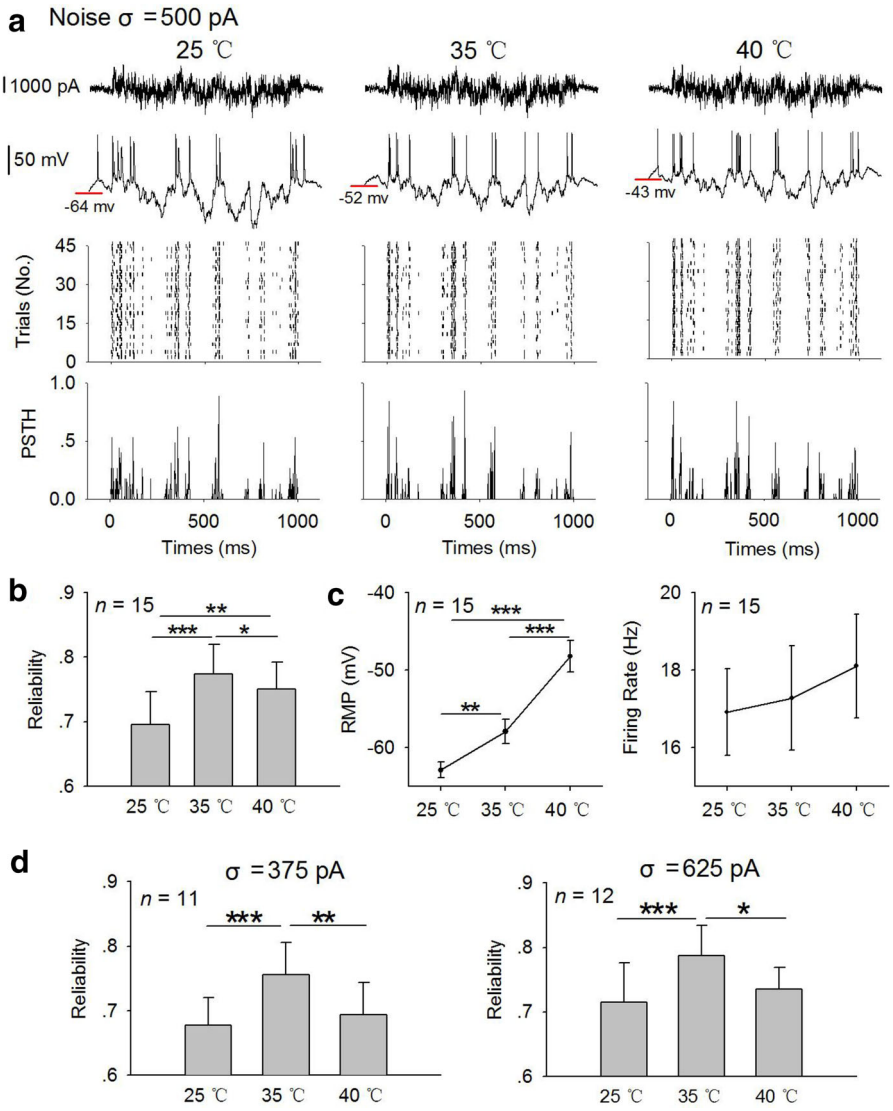

Fig. 1 Neuronal response reliability was maximal at PT. **a** Input signals ($\sigma = 500$ pA), representative neuronal responses, neuronal raster plots of firing timings and PSTHs from 45 trials at RT (left panel), PT (middle panel) and HT (right panel), showing that the neuron displayed more reproducible responses to repeated noise signals at PT than at RT and HT. The membrane potential depolarized as the temperature increased, as shown by the red line, **b** paired comparisons of spiking reliability at RT, PT and HT in response to repeated input signals with a σ of 500 pA, showing that the spiking reliability exhibited a global maximum when the temperature was PT, **c** the RMP depolarized and firing rate increased as the temperature increased from RT to HT, **d** same analyses as presented in **b**, with the exception of the noise intensities, which were 375 and 625 pA, respectively. $^{*}p < 0.05$; $^{**}p < 0.01$; $^{***}p < 0.001$, paired *t* test, *n* represented the number of neurons analyzed in this experiment. (Color figure online)

of 250, 500 and 625 pA were chosen (Fig. 2a). The neuronal firing rate increased as the noise intensity increased (4.46 ± 0.50 at 250 pA; 12.62 ± 0.91 at 500 pA; and 18.41 ± 1.26 at 625 pA; $p < 0.001$ for the comparison between 250 pA, 500 pA and 625 pA; paired *t* test; $n = 14$; Fig. 2d). Under this condition, we maintained the neuronal membrane potential at the same level (− 57.38 ± 1.07 mV at 250 pA; − 57.44 ± 1.11 mV at 500 pA; − 57.14 ± 1.34 mV at 625 pA; Fig. 2c and red line in Fig. 2a). The raster plots and corresponding PSTHs from 45 trials showed an effect of noise intensity on increasing the response reproducibility (Fig. 2a). Based on the results from the statistical analyses, the neuron displayed the maximum reliability when injected with a signal with a stronger intensity (0.65 ± 0.04 at 250 pA, 0.76 ± 0.05 at 500 pA and 0.78 ± 0.05 at 625 pA; $p < 0.01$ for the comparison between 250 pA, 500 pA and 625 pA; paired *t* test; $n = 14$; Fig. 2b).

Second, we explored the effects of the neuronal membrane potential on spiking reliability. A direct current (DC) injection was used to adjust the membrane potential to different levels, e.g., RMP (− 61.61 ± 1.36 mV), depolarization (− 51.29±1.26 mV) or hyperpolarization (− 70.93 ± 1.41 mV; Fig. 3b and red lines in Fig. 3a). The firing rate was maintained at approximately equal value at various membrane potentials (11.64 ± 0.59 at − 71 mV, 10.86 ± 0.44 at − 62 mV and

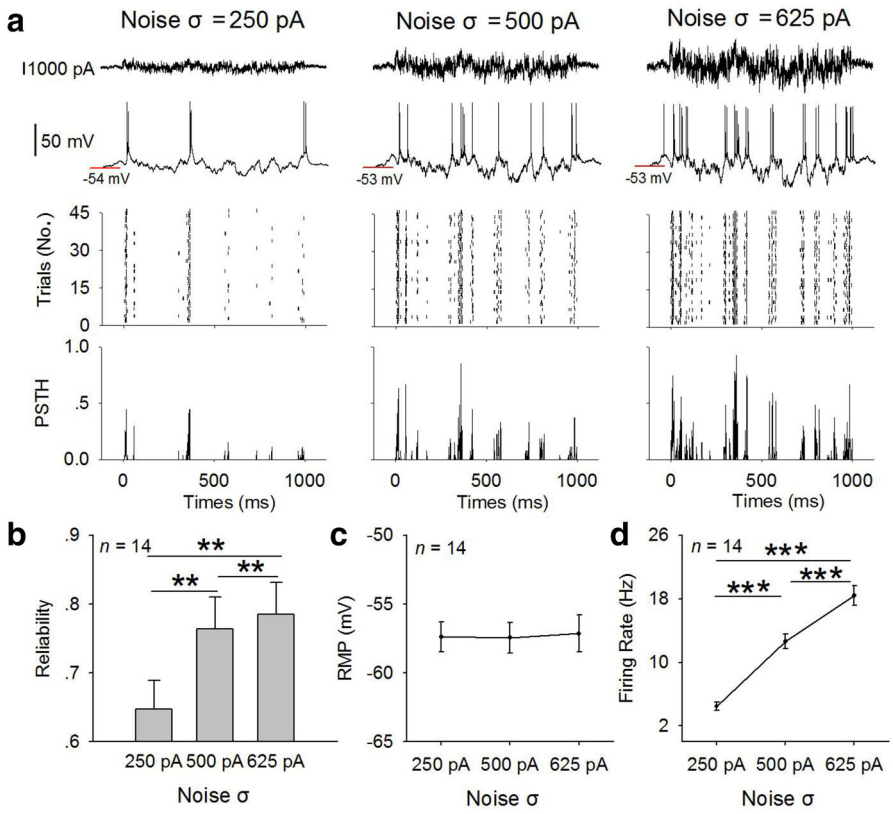

Fig. 2 Dependence of the response reliability on the stimulus intensity. **a** Input signals, representative neuronal responses, neuronal raster plots of firing timings and PSTHs from 45 trials at noise intensities of 250 pA (left panel), 500 pA (middle panel) and 625 pA (right panel). The membrane potential was maintained at the RMP, as shown by the red line, **b** paired comparisons of spiking reliability at different noise intensities, showing that the neuron displayed the maximum reliability when injected with a signal with a stronger intensity. RMP (**c**) and firing rate (**d**) of neurons at different noise intensities. $*p < 0.05$; $**p < 0.01$; $***p < 0.001$, paired *t* test, *n* represented the number of neurons analyzed in this experiment. (Color figure online)

10.40 ± 0.47 at -51 mV; Fig. 3c) by introducing noise stimuli of various intensities (250–750 pA). Representative responses, spike timing rasters and PSTHs at various membrane potentials were plotted, and the maximum response repeatability was observed at a hyperpolarized membrane potential (Fig. 3a). According to the statistical analyses, neurons displayed higher response reliability at -71 mV (0.79 ± 0.05) than at -51 mV (0.71 ± 0.05) or -62 mV (0.75 ± 0.05) ($p < 0.001$ for the comparison between -71 and -62 mV and $p < 0.001$ for the comparison between -71 and -51 mV; paired *t* test; $n = 16$) under the condition of controlled firing rate (Fig. 3b, c). Moreover, we also studied the spiking reliability at various membrane potentials with the same noise intensity (500 pA). Similar to the injection of noise stimuli with unequal intensities, the spiking reliability was significantly higher at -72 mV (0.79 ± 0.07) than at -62 mV (0.77 ± 0.07; $p < 0.05$; paired *t* test; $n = 8$; Fig. 3d) though the firing rate was low at -72 mV (7.53 ± 1.28 at -72 mV, 15.04 ± 0.83 at -62 mV and 20.49 ± 0.81 at -53 mV; $p < 0.01$ for the comparison between -72 mV and -62 mV and $p < 0.001$ for the comparison between -62 mV and -53 mV; paired *t* test; $n = 8$; Fig. 3e).

Based on these results, a relatively hyperpolarized membrane potential and relatively strong stimulus intensity contributed to a large response reliability. At PT with the same stimulus intensity, the RMP and response reliability of cortical neurons were higher than at RT, suggesting that the higher response reliability at PT was dominated by other factors.

3.3 The maximal response reliability might be due to the optimal balance of excitation and inhibition in the networks at PT

The neuronal response reliability to an input signal is always altered by the surrounding network modulations, particularly the balance of network excitation and inhibition (E/I balance) [43–46]. Temperature fluctuations may shift the E/I balance and change the neuronal response reliability. We recorded the responses of pyramidal neurons and PV interneurons to a DC current injection (500 pA, 500 ms) under different tem-

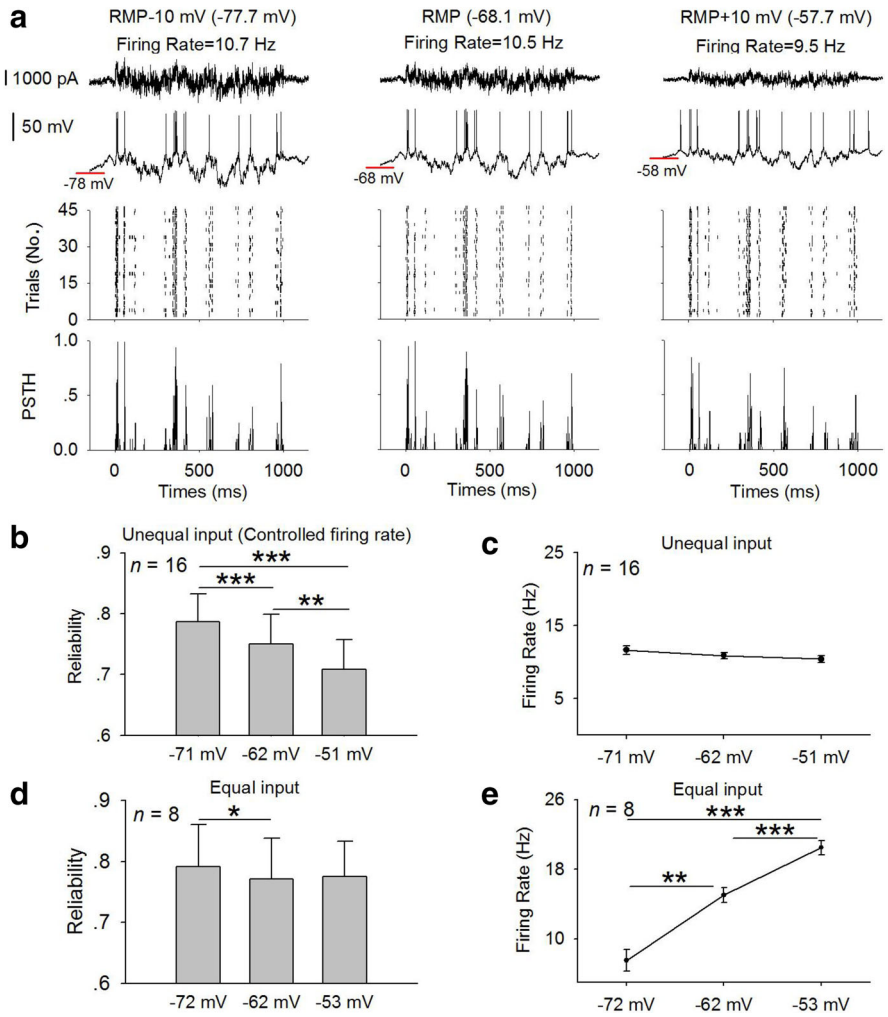

Fig. 3 Dependence of the response reliability on the RMP level. **a** Input signals, representative neuronal responses, neuronal raster plots of firing timings and PSTHs from 45 trials at −78 mV (left panel), −68 mV (middle panel) and −58 mV (right panel). The membrane potentials were indicated by the red lines. The noise intensity of the input signals had five grades (250, 375, 500, 625 and 750 pA) to ensure an approximately identical firing rate at various membrane potentials, as shown in **c**, **b** paired comparisons of spiking reliability at various membrane potentials under the condition of an equal firing rate (the firing rates was shown in **c**), showing that the neuron displayed the maximum reliability at a hyperpolarized membrane potential, **c** equal firing rate of neurons at different membrane potentials (unequal input), **d** paired comparisons of spiking reliability at various membrane potentials under the condition of the injection of noise with an equal intensity, **e** firing rate of neurons at different membrane potentials (equal input). Though the firing rate was low at a hyperpolarized membrane potential, the response reliability was high. $*p < 0.05$; $**p < 0.01$ and $***p < 0.001$, paired t test, n represented the number of neurons analyzed in this experiment. (Color figure online)

perature conditions, namely RT, PT and HT, to test this hypothesis (Fig. 4a). The mean firing rate of pyramidal neurons increased gradually (30.68 ± 0.95 Hz at RT, 39.35 ± 1.68 Hz at PT and 42.07 ± 1.92 Hz at HT; $p < 0.001$ for the comparison between RT, PT and HT; paired t test; $n = 42$; Fig. 4b) as the temperature increased from RT to HT, while the mean firing rate of PV interneurons decreased (127.90 ± 5.62 Hz at RT, 74.10 ± 16.60 Hz at PT and 52.48 ± 18.13 Hz at HT; $p < 0.001$ for the comparison between RT and HT and $p < 0.01$ for the comparison between RT and PT; paired t test; $n = 21$; Fig. 4b). The ratio of the mean firing rate between pyramidal neurons and PV interneurons increased from 0.24 at RT to 0.53 at PT

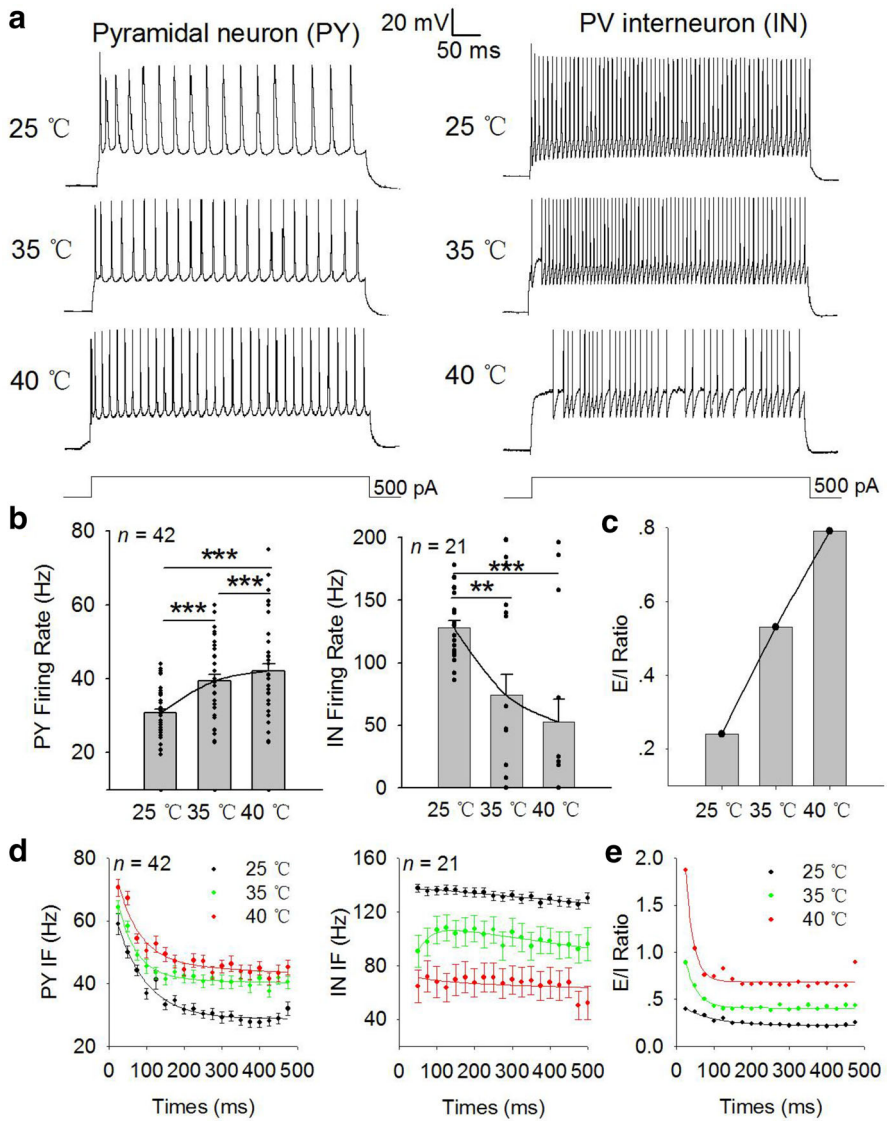

Fig. 4 Temperature fluctuations altered the E/I balance. **a** Representative spiking patterns of pyramidal neurons (left panel) and PV interneurons (right panel) in response to a DC current injection (500 pA; 500 ms) at RT, PT and HT, **b** paired comparisons of the mean firing rate of pyramidal neurons and interneurons at RT, PT and HT. The curves indicated the increased firing rate of pyramidal neurons and decreased firing rate of interneurons as the temperature increased, **c** the ratio of firing rate between pyramidal neurons and PV interneurons (E/I ratio) showed an increase as temperature increased, as shown in the curve, **d** IF of pyramidal neurons and interneurons during a 500 ms stimulus duration at RT, PT and HT, **e** the ratio of IF between pyramidal neurons and PV interneurons (E/I ratio) showed an increase as temperature increased during a 500 ms stimulus duration. $*p < 0.05$; $**p < 0.01$; $***p < 0.001$, paired *t* test, *n* represented the number of neurons analyzed in this experiment

(Fig. 4c). The instantaneous frequency (IF) displayed the same trends as the mean firing rate. As the temperature increased, the IF increased for pyramidal neurons and decreased for interneurons during the 500 ms stimulus duration (Fig. 4d). The ratio of IF between pyramidal neurons and interneurons increased as the temperature increased (Fig. 4e). Compared with RT, a clear increase in the E/I balance toward excitation was observed at PT and HT. The E/I balance observed at PT might be the optimal condition to maximize the spiking reliability since excess excitation might occur at HT.

3.4 The contributions of Na^+ and K^+ ion channels to the neuronal response reliability

The random gating of voltage-gated ion channels may be critical for determining the spiking reliability [6]. We evaluated the contributions of Na^+ and K^+ ion channels to the neuronal response reliability by partially blocking Na^+ or K^+ channels, respectively. The effects of 4-AP on the shape of AP waveforms were shown in Fig. 5c. The partial inhibition of K^+ channels broadened the AP half-duration (2.51 ± 0.11 ms

vs 3.05 ± 0.14 ms at RT, $p < 0.001$, $n = 10$; 1.02 ± 0.04 ms vs 1.28 ± 0.06 ms at PT, $p < 0.001$, $n = 17$; 0.73 ± 0.08 ms vs 0.81 ± 0.05 ms at HT, $p > 0.05$, $n = 7$; paired t test) and decreased the dV/dt ratio (|min dV/dt|/max dV/dt) (0.24 ± 0.01 vs 0.17 ± 0.01 at RT, $p < 0.001$, $n = 10$; 0.28 ± 0.01 vs 0.24 ± 0.01 at PT, $p < 0.001$, $n = 17$; 0.38 ± 0.01 vs 0.32 ± 0.02 at HT, $p < 0.01$, $n = 7$; paired t test) and firing rate (16.50 ± 1.35 Hz vs 12.40 ± 1.32 Hz at RT, $p < 0.001$, $n = 10$; 18.08 ± 1.25 Hz vs 14.58 ± 1.17 Hz at PT, $p < 0.001$, $n = 17$; 19.87 ± 1.71 Hz vs 14.72 ± 0.95 Hz at HT, $p < 0.05$, $n = 7$; paired t test; Fig. 5c). Importantly, K^+ channels played an important role in determining the response reliability. Compared with control conditions, 4-AP decreased the neuronal response repeatability (Fig. 5a) and the values of response reliability at all the tested temperatures (0.70 ± 0.07 vs 0.64 ± 0.06 at RT, $p < 0.001$, $n = 10$; 0.76 ± 0.04 vs 0.70 ± 0.04 at PT, $p < 0.001$, $n = 17$; 0.74 ± 0.06 vs 0.69 ± 0.06 at HT, $p < 0.05$, $n = 7$; paired t test; Fig. 5b), and the values recovered after washout. The partial inhibition of Na^+ channels exerted the opposite effects on the shape of AP waveforms (Fig. 6c). TTX application decreased the AP half-duration (2.38 ± 0.11 ms vs 2.05 ± 0.16 ms at RT, $p < 0.05$, $n = 10$; 1.09 ± 0.04 ms vs 1.03 ± 0.04 ms at PT, $p = 0.09$, $n = 18$; 0.86 ± 0.16 ms vs 0.74 ± 0.05 ms at HT, $p > 0.05$, $n = 8$; paired t test) and number of APs (13.95 ± 1.49 Hz vs 8.99 ± 1.01 Hz at RT, $p < 0.001$, $n = 10$; 15.71 ± 1.23 Hz vs 8.61 ± 0.88 Hz at PT, $p < 0.001$, $n = 18$; 17.57 ± 2.89 Hz vs 7.72 ± 1.27 Hz at HT, $p < 0.01$, $n = 8$; paired t test), but increased the dV/dt ratio (0.26 ± 0.03 vs 0.30 ± 0.02 at RT, $p > 0.05$, $n = 10$; 0.28 ± 0.01 vs 0.31 ± 0.01 at PT, $p < 0.01$, $n = 18$; 0.33 ± 0.03 vs 0.36 ± 0.03 at HT, $p > 0.05$, $n = 8$; paired t test; Fig. 6c). Consistent with the effects of K^+ channels, the partial inhibition of Na^+ channels decreased the neuronal response repeatability (Fig. 6a) and the values for reliability at PT (0.72 ± 0.07 vs 0.69 ± 0.06 at RT, $p > 0.05$, $n = 10$; 0.76 ± 0.04 vs 0.72 ± 0.05 at PT, $p < 0.01$, $n = 18$; 0.73 ± 0.06 vs 0.71 ± 0.06 at HT, $p > 0.05$, $n = 8$; paired t test; Fig. 6b). The results showed that the reduction of either K^+ or Na^+ channel conductance reduced the response reliability of the neurons.

3.5 The maximum information transmission rate and coding efficiency of neurons were observed at PT

We introduced two information measures, information transmission rate and coding efficiency (see Sect. 2.4) to verify the hypothesis that the information transmission was more efficient by cortical pyramidal neurons at PT than at RT and HT. After changing the temperature from RT to HT ($n = 14$ at RT, $n = 26$ at PT, $n = 14$ at HT), the smallest total response entropy H_{total} was recorded at HT (83.61 ± 3.33 bits/s) ($p < 0.01$ for the comparison between RT and HT; paired t test) compared with RT (99.57 ± 3.89 bits/s) and PT (89.98 ± 3.35 bits/s; Fig. 7b), the minimal noise entropy H_{noise} was recorded at PT (21.96 ± 1.08 bits/s) ($p < 0.001$ for the comparison between RT and PT and $p < 0.001$ for the comparison between PT and HT; paired t test) compared with RT (31.33 ± 2.84 bits/s) and HT (34.87 ± 2.61 bits/s; Fig. 7c), and the smallest mutual information MI was recorded at HT (48.74 ± 4.17 bits/s) ($p < 0.01$ for the comparison between RT and HT and $p < 0.001$ for the comparison between PT and HT; paired t test) compared with RT (68.24 ± 2.76 bits/s) and PT (68.03 ± 2.98 bits/s; Fig. 7d). These results suggested that the information in the response related to the stimulus was smallest in HT. Figure 7a showed that compared with RT ($n = 14$) and HT ($n = 14$), the highest values of the coding efficiency (0.69 ± 0.02 at RT, 0.75 ± 0.01 at PT and 0.57 ± 0.03 at HT; $p < 0.01$ for the comparison between RT and PT and $p < 0.001$ for the comparison between PT and HT; paired t test) and information transmission rate (2.52 ± 0.11 bits/spike at RT, 3.57 ± 0.11 bits/spike at PT and 2.93 ± 0.18 bits/spike at HT; $p < 0.001$ for the comparison between RT and PT and $p < 0.01$ for the comparison between PT and HT; paired t test) of neurons were observed at PT ($n = 26$). Thus, each AP carried more information, the neuronal activities required to encode and transmit the input signal were more efficient at PT.

3.6 Computational simulations confirmed maximal neuronal response reliability and coding efficiency at PT

We carried out computational simulations of a HH cortical neuronal model to evaluate the spike timing reliability of the model neuron based on the evoked spike

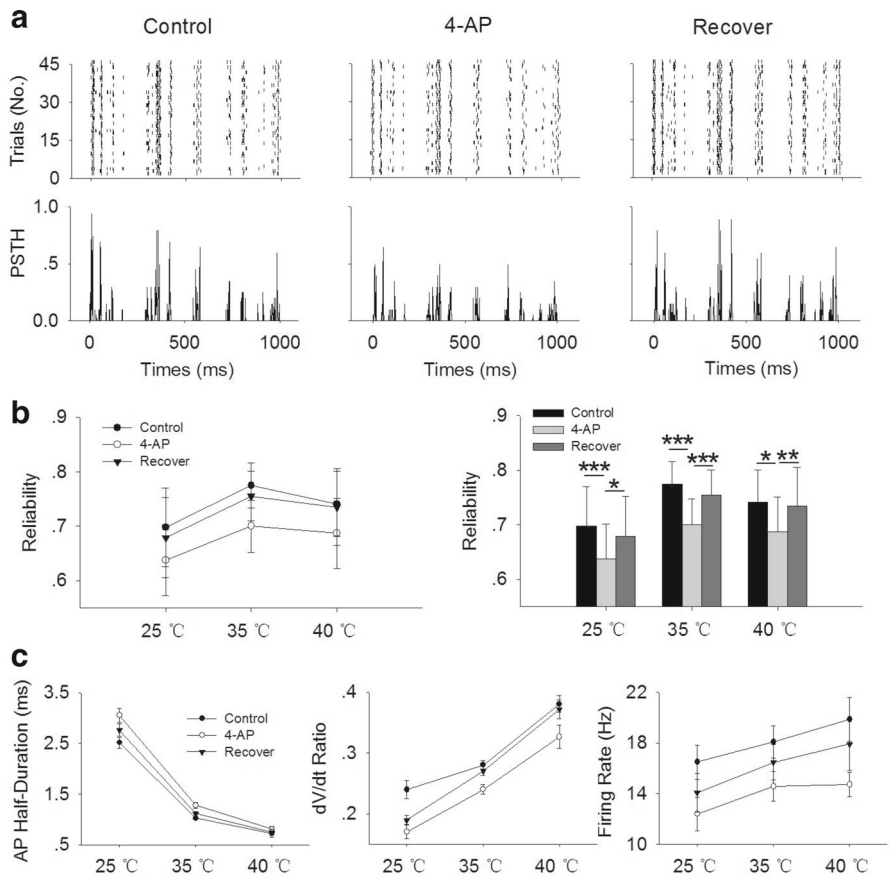

Fig. 5 Effects of the partial inhibition of K^+ channels on the response reliability and shape of AP waveforms in pyramidal neurons. **a** Neuronal raster plots and PSTHs from 45 trials were plotted under normal condition, in the presence of 1 mM 4-AP, and recovered after washout, respectively, **b** line charts and bar plots showed paired comparisons of the response reliability at RT, PT and HT under normal condition, in the presence of 1 mM 4-AP, and recovered after washout. 4-AP decreased the neuronal response reliability at all the tested temperatures, **c** the AP half-duration (left panel), dV/dt ratio (middle panel) and firing rate (right panel) were plotted under normal condition, in the presence of 1 mM 4-AP, and recovered after washout at RT, PT and HT. 4-AP broadened the AP half-duration and decreased the dV/dt ratio and firing rate. $^*p < 0.05$; $^{**}p < 0.01$; $^{***}p < 0.001$, paired t test

trains by injecting signals repeatedly at RT, PT and HT, respectively. Consistent with the experimental observations, the firing rate increased as the temperature increased (Fig. 8b). The model neuron displayed more reproducible responses at PT than at RT and HT according to the raster plots and PSTHs shown in Fig. 8a. Further quantitative analysis demonstrated that the reliability of the model neuron was 0.56 ± 0.003 at PT, which was significantly greater than at RT (0.49 ± 0.01) and HT (0.40 ± 0.003) conditions (Fig. 8b).

To evaluate the contributions of Na^+ and K^+ ion channels to the neuronal response reliability, we decreased g_{Na}^{max} or g_K^{max} in a systematical way. Figure 8c shows example results of response reliability for $g_{Na}^{max} = 1500$ and 900 pS/μm^2, $g_K^{max} = 60$ and 30 pS/μm^2 at RT, PT and HT, respectively. Consistent with the experimental effects, the decrease of either g_{Na}^{max} or g_K^{max} decreased the response repeatability (g_{Na}^{max}: 0.49 ± 0.01 vs 0.37 ± 0.01 at RT, 0.56 ± 0.003 vs 0.45 ± 0.01 at PT, 0.40 ± 0.003 vs 0.25 ± 0.003 at HT; g_K^{max}: 0.49 ± 0.01 vs 0.48 ± 0.002 at RT, 0.56 ± 0.003 vs 0.51 ± 0.01 at PT, 0.40 ± 0.003 vs 0.33 ± 0.004 at HT; Fig 8c).

We then calculated the information transmission rate and coding efficiency of the model neuron at different conditions. The total response entropy H_{total} increased

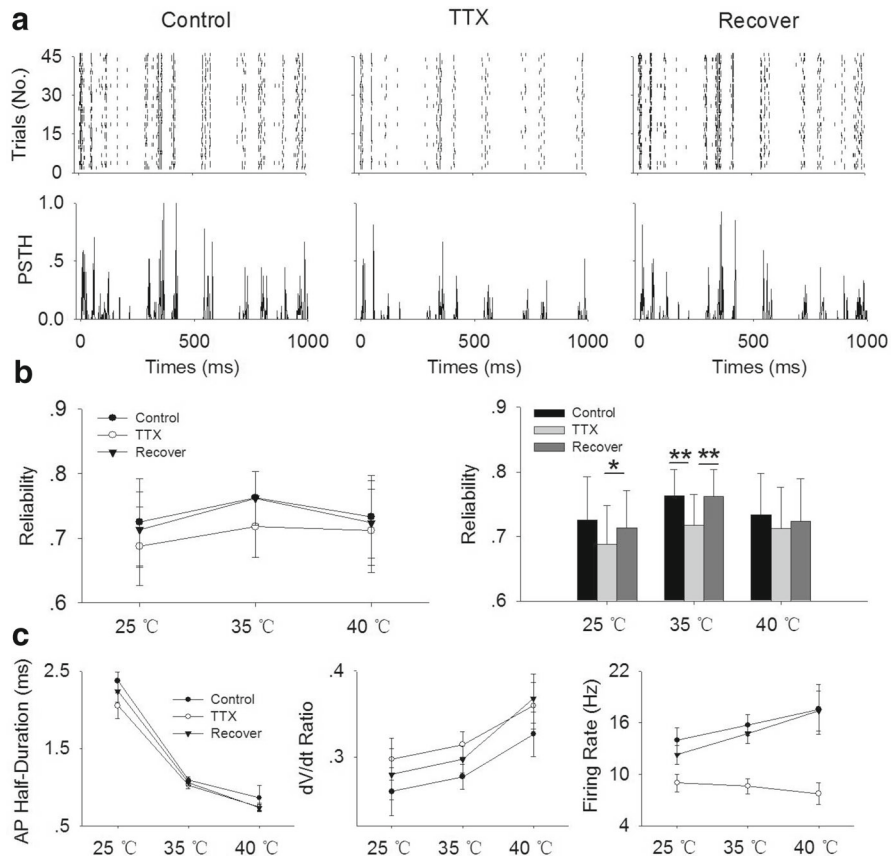

Fig. 6 Effects of the partial inhibition of Na^+ channels on the response reliability and shape of AP waveforms in pyramidal neurons. **a** Neuronal raster plots and PSTHs from 45 trials were plotted under normal condition, in the presence of 10 nM TTX, and recovered after washout, respectively, **b** line charts and bar plots showed paired comparisons of the response reliability at RT, PT and HT under normal condition, in the presence of 10 nM TTX, and recovered after washout. TTX decreased the neuronal response reliability at PT, **c** AP half-duration (left panel), d*V*/d*t* ratio (middle panel) and firing rate (right panel) were plotted under normal condition, in the presence of 10 nM TTX, and recovered after washout at RT, PT and HT. TTX decreased the AP half-duration and firing rate, broadened the d*V*/d*t* ratio. $*p < 0.05$; $**p < 0.01$; $***p < 0.001$, paired *t* test

with the increase in temperature (77.93 ± 3.89 bits/s at PT, 98.35±1.16 bits/s at RT, 116.44±3.07 bits/s at HT; Fig. 9b). The noise entropy H_{noise} was minimal at PT (42.48 ± 1.29 bits/s) than at RT (45.72 ± 1.45 bits/s) and at HT (79.55 ± 1.96 bits/s; Fig. 9c). The mutual information MI was highest at PT (32.21 ± 4.08 bits/s at RT, while it was 55.87 ± 1.80 bits/s at PT and 36.88±3.20 bits/s at HT; Fig. 9d). Similar to the experimental results, Fig. 9a showed that the coding efficiency (0.41 ± 0.03 at RT, 0.56 ± 0.01 at PT, 0.32 ± 0.02 at HT) and information transmission rate (2.63 ± 0.34 bits/spike at RT, 3.98±0.13 bits/spike at PT, 2.19± 0.19 bits/spike at HT) were highest at PT. The results suggested that the body temperature was crucial for efficient information coding and transmission in a realistic neuronal model whose biophysical properties were validated by previous experimental studies [35,40].

4 Discussion and conclusions

As a result of evolution, birds and mammals develop a constant warm body temperature, which is indeed costly in terms of metabolic consumption. In this paper, we studied the functional benefits of body temperature for cortical coding and response reliability by a combination of in vitro whole-cell patch clamp recordings and computational simulations of HH cortical neu-

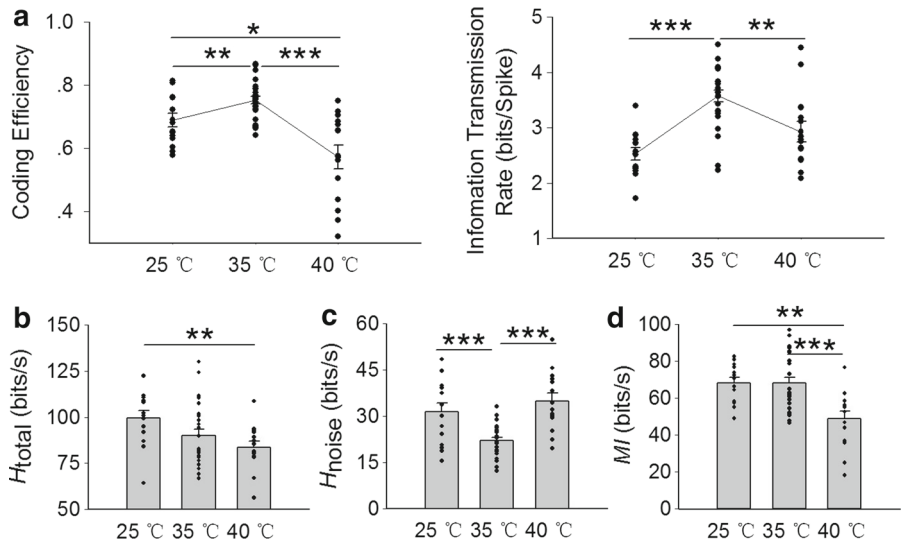

Fig. 7 **a** Paired comparisons of the coding efficiency and information transmission rate of pyramidal neurons at RT, PT and HT. The coding efficiency and information transmission rate were highest at PT. Paired comparisons of the H_{total} (**b**), H_{noise} (**c**) and MI (**d**) of pyramidal neurons at RT, PT and HT. $^{*}p < 0.05$; $^{**}p < 0.01$; $^{***}p < 0.001$, paired *t* test

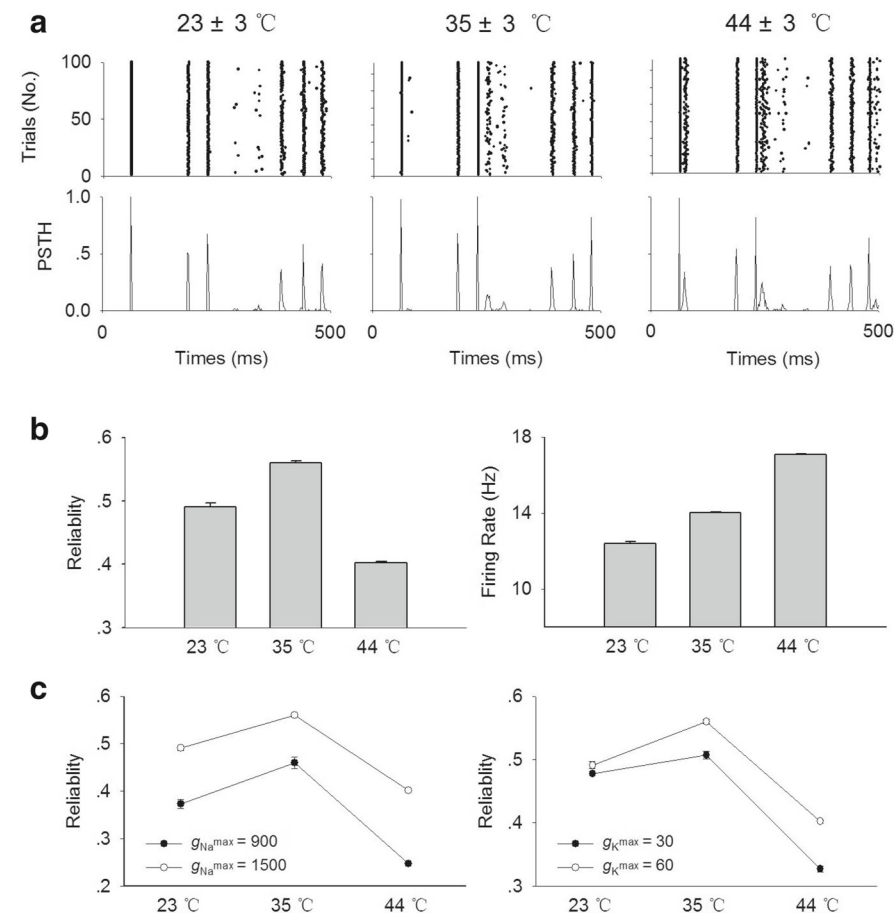

Fig. 8 Computational simulations revealed maximal neuronal response reliability at PT. **a** Model neuronal raster plots of firing timings and PSTHs from 100 trials at three temperature conditions, **b** calculated spiking reliability and firing rate at different temperatures in response to repeated input signal. The spiking reliability was maximum when the temperature was PT, **c** effect of decrease of $g_{\text{Na}}^{\text{max}}$ and $g_{\text{K}}^{\text{max}}$ on the response reliability. The decrease of either Na^{+} channel or K^{+} channel decreased the neuronal response reliability at all the tested temperatures

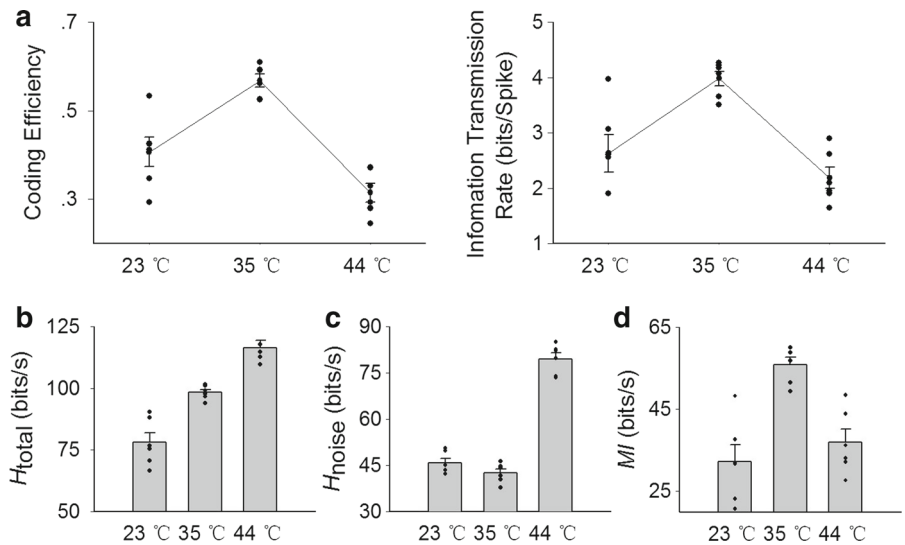

Fig. 9 Computational simulations revealed maximal information transmission rate and coding efficiency at PT. **a** Calculated coding efficiency and information transmission rate of model neuron at different temperatures, showing that the coding efficiency and information transmission rate were highest at PT. Calculated total response entropy H_{total} (**b**), noise entropy H_{noise} (**c**) and mutual information MI (**d**) of model neuron at three temperature conditions

ronal model. This study provided the first experimental evidence that the neuronal response reliability, coding efficiency and information transmission rate of cortical pyramidal neurons reached the maximal level at the physiological body temperature compared with low-temperature (e.g., RT) and high-temperature (e.g., HT) conditions. Also, the experimental results were further reproduced and validated by the numerical simulations of a computational neuronal model. The physiological body temperature might be corresponding to an optimal level of the network excitation and inhibition, which were one of the key factors underlying cortical response reliability. The temperature fluctuations may impair the efficiency and reliability of neuronal information processing [7,47]. The precision of the spike timing is critical for the reliable propagation of the neuronal response, as spike timing with larger jitters does not propagate over a long distance in multilayered feedforward networks [48,49]. Therefore, based on the results, maintaining a constant body temperature is crucial for protection of reliable and most efficient information coding and transmission in complex cortical circuits.

Multiple factors may contribute to the maximal cortical spike timing reliability at physiological body temperature. Our experimental recordings of pyramidal neurons showed that a higher stimulus intensity or relatively hyperpolarized membrane potential increased the response reliability. Within the same stimulus intensity condition, pyramidal neurons showed a gradual increase in the firing rate and depolarization of the membrane potential as the temperature increased (Fig. 1c). Hence, the maximal response reliability observed at PT was definitely not due to changes in the membrane potential. In addition, a higher firing rate was recorded at HT than at PT, while a lower response reliability was recorded at HT than at PT. Hence, the firing rate was also not a critical factor contributing to the maximal response reliability observed at PT.

Cortical computations are performed through the precise modulations of synaptic excitation and inhibition patterns at the network level [45,50]. The functional architectures may serve to sharpen the spike timing precision in response to fluctuating components in the input signal [51]. According to a recent experimental study, an increase in synaptic conductance and a shift in the E/I balance toward excitation may contribute to the enhanced trial-to-trial reliability during locomotion and attention [46]. Balanced changes in excitatory and inhibitory inputs during repetitive whisker deflection could preserve the narrow time windows of spike generation in layer 4 of the rat barrel cortex [52]. In the present study, the ratio of the mean firing rate or instantaneous firing rate between pyramidal neurons and PV interneurons increased as the temperature increased. These findings suggested a shift in the E/I balance toward excitation at PT, which might serve to enhance the response reliability at PT. At HT, the E/I balance might be excessively shifted toward excitation, potentially led to hyperexcitability and disrupted neuronal functions. This mechanism likely underlay the genesis of febrile seizures (FS). The optimal balance between excitation and inhibition at PT may be the basis of

normal brain activity, and an imbalance will induce brain disorders and unreliable neuronal information processing.

Intrinsic neuronal properties, such as the distribution of ion channels, are also key factors contributing to the electrical responses of neurons. The difference in spiking reliability in response to signals of various frequencies between pyramidal neurons and interneurons is reported to be caused by the different compositions of ion channels [13]. Changes in ion channels may provide a useful way for neurons to maximize spiking reliability. According to conductance-based models of cortical neurons, neurons with larger and faster slow K^+ currents exhibit more reliable spike timing; however, a larger persistent Na^+ current impairs reliability, suggesting that both channel types significantly influence spike reliability [53]. In addition, ion channel stochasticity causes channel noises [6]. Regarding the total numbers (N) of channels and open probability (p) of each channel, the size of the noisy current is the square root of $(1-p)/Np$. If N decreases as following the partial blockade of Na^+ or K^+ channels, the channel noise may dominate the randomness of the resulting spikes generated. In this situation, the blockade of Na^+ or K^+ channels results in a decreased response reliability, consistent with the results of our experiments and models. In the present study, partial blockade of either Na^+ or K^+ channels noticeably changed the shape of AP waveforms and decreased the neuronal response reliability. The results suggested that both K^+ channel conductance and Na^+ channel conductance were important factors in regulating the neuronal response reliability, and their kinetics might be in the optimal balance in normal body temperature conditions corresponding to the maximal firing reliability.

The simulations results revealed that the response reliability, information transmission rate and coding efficiency also went through a global maximum when the temperature was at around $35 \pm 3\,^{\circ}C$. This was consistent with the experimental observations and suggested that the kinetics and dynamics of the action potential generation in cortical neurons may have the best performance at around physiological temperature in warm-blooded animals. The kinetics and biophysical parameters of this HH neuronal model were all derived from the validations of experimental observations of action potential properties in layer V/VI pyramidal neurons of mammalian brains. In normal condition, both sodium channel conductance and potassium channel conductance are in the optimal balance with appropriate ratio. Once the conductance of either sodium or potassium channel is reduced, the neuronal response reliability drops quickly, as demonstrated in Fig. 8. For the lower temperature than the physiological body temperature, the kinetics of ionic channels become slower and the time constants of both sodium and potassium increase to be several times longer than in physiological temperature, which slows down the neuronal excitation process and decreases the firing rate [35]. Correspondingly, the firing reliability is reduced. For the higher temperature than the physiological temperature, the kinetics and dynamics of the ionic channels are increased rapidly, and the neuronal excitability is also increased, leading to a higher firing rate [35]. The speeding up of the action potential process may result in abnormal and unreliable firing excitability, which may even induce epileptic waveform [54]. Therefore, there may exist an optimal kinetics for both sodium channels and potassium channels in the mammalian cortical neurons within the range of body temperature, which may be developed during the long-term natural evolution.

In conclusion, the temperature fluctuations may substantially affect the spiking response reliability, coding efficiency and information transmission rate of cortical neurons. The cortical coding process may have already adapted to the physiological body temperature, and cortical performance is set to the optimal level. Any dramatic decrease or increase in temperature may shift the optimal balance between neuronal excitation and inhibition in the network, resulting in abnormal cortical functions and unreliable cortical coding. Maintaining a constant body temperature may be beneficial to ensure the precise cortical computations and reliable spiking transmissions that are the bases for constructing delicate cortical circuits.

Acknowledgements YY thanks for the support from the National Natural Science Foundation of China (81761128011, 31571070), the Shanghai Municipal Science and Technology Major Project (No. 2018SHZDZX01) and ZJLab, the Shanghai Science and Technology Committee support (16410722600), and the program for the Professor of Special Appointment (Eastern Scholar SHH1140004) at Shanghai Institutions of Higher Learning.

Author contributions YY supervised the research, YY and XF designed the research, XF and YY performed the experimental study and data analysis, and XF and YY wrote the paper. All authors reviewed the manuscript.

Compliance with ethical standards

Conflict of interest The authors declare that there is no conflict of interest regarding the publication of this article.

Human and animal statement The conducts and procedures involving animal experiments in this study were approved by the Animal Ethics Committee of Fudan University School of Life Sciences.

References

1. Van Rossum, M.C., O'Brien, B.J., Smith, R.G.: Effects of noise on the spike timing precision of retinal ganglion cells. J. Neurophysiol. **89**(5), 2406–2419 (2003)
2. Movshon, J.A.: Reliability of neuronal responses. Neuron **27**(3), 412–414 (2000)
3. Cudmore, R.H., Fronzaroli-Molinieres, L., Giraud, P., Debanne, D.: Spike-time precision and network synchrony are controlled by the homeostatic regulation of the D-type potassium current. J. Neurosci. **30**(38), 12885 (2010)
4. Mainen, Z.F., Sejnowski, T.J.: Reliability of spike timing in neocortical neurons. Science **268**(5216), 1503–1506 (1995)
5. Mcadams, C.J., Maunsell, J.H.R.: Effects of attention on the reliability of individual neurons in monkey visual cortex. Neuron **23**(4), 765–773 (1999)
6. Schneidman, E., Freedman, B., Segev, I.: Ion channel stochasticity may be critical in determining the reliability and precision of spike timing. Neural Comput. **10**(7), 1679–1703 (1998)
7. Yu, Y.G.: Constant warm body temperature ensures high response reliability of neurons in endothermic brains. Austin J. Comput. Biol. Bioinf. **1**(1), 5 (2014)
8. Ermentrout, G.B., Galán, R.F., Urban, N.N.: Reliability, synchrony and noise. Trends Neurosci. **31**(8), 428–434 (2008)
9. Thiele, A., Herrero, J.L., Distler, C., Hoffmann, K.P.: Contribution of cholinergic and GABAergic mechanisms to direction tuning, discriminability, response reliability, and neuronal rate correlations in macaque middle temporal area. J. Neurosci. **32**(47), 16602 (2012)
10. Guo, D.Q., Perc, M., Liu, T.J., Yao, D.Z.: Functional importance of noise in neuronal information processing. Europhys. Lett. **124**(5), 50001 (2018)
11. Gammaitoni, L., Hänggi, P., Jung, P., Marchesoni, F.: Stochastic resonance. Rev. Mod. Phys. **70**(1), 223 (1998)
12. Yu, Y.G., Wang, W., Wang, J.F., Liu, F.: Resonance-enhanced signal detection and transduction in the Hodgkin–Huxley neuronal systems. Phys. Rev. E **63**(2), 12 (2001)
13. Fellous, J., Houweling, A., Modi, R., Rao, R., Tiesinga, P., Sejnowski, T.: Frequency dependence of spike timing reliability in cortical pyramidal cells and interneurons. J. Neurophysiol. **85**(4), 1782–1787 (2001)
14. Yu, Y.G., Liu, F., Wang, J., Wang, W.: Spike timing precision for a neuronal array with periodic signal. Phys. Lett. A **282**(1–2), 23–30 (2001)
15. Zhu, Y.J., Qiao, W.H., Liu, K.F., Zhong, H.Y., Yao, H.S.: Control of response reliability by parvalbumin-expressing interneurons in visual cortex. Nat. Commun. **6**(1), 6802–6802 (2014)
16. Guo, D.Q., Chen, M.M., Perc, M., Wu, S.D., Xia, C., Zhang, Y.S., Xu, P., Xia, Y., Yao, D.Z.: Firing regulation of fast-spiking interneurons by autaptic inhibition. Europhys. Lett. **114**(3), 30001 (2016)
17. Guo, D.Q., Wu, S.D., Chen, M.M., Perc, M., Zhang, Y.S., Ma, J.L., Cui, Y., Xu, P., Xia, Y., Yao, D.Z.: Regulation of irregular neuronal firing by autaptic transmission. Sci. Rep. **6**, 26096 (2016)
18. Gosak, M., Markovič, R., Dolenšek, J., Rupnik, M.S., Marhl, M., Stožer, A., Perc, M.: Network science of biological systems at different scales: a review. Phys. Life Rev. **24**, 118–135 (2018)
19. Bera, B.K., Majhi, S., Ghosh, D., Perc, M.: Chimera states: effects of different coupling topologies. Europhys. Lett. **118**(1), 10001 (2017)
20. Majhi, S., Bera, B.K., Ghosh, D., Perc, M.: Chimera states in neuronal networks: a review. Phys. Life Rev. **28**, 100–121 (2018)
21. Yu, Y.G., Liu, F., Wang, W., Lee, T.S.: Optimal synchrony state for maximal information transmission. Neuroreport **15**(10), 1605–1610 (2004)
22. Reig, R., Mattia, M., Compte, A., Belmonte, C., Sánchez-Vives, M.V.: Temperature modulation of slow and fast cortical rhythms. J. Neurophysiol. **103**(3), 1253–1261 (2009)
23. Hedrick, T., Waters, J.: Spiking patterns of neocortical L5 pyramidal neurons in vitro change with temperature. Front. Cell. Neurosci. **5**(3), 1 (2011)
24. Andersen, P., Moser, E.I.: Brain temperature and hippocampal function. Hippocampus **5**(6), 491–498 (1995)
25. Jerison, H.J.: Paleoneurology and the evolution of mind. Sci. Am. **234**(1), 90–101 (1976)
26. Hamilton, C.L., Ciaccia, P.J.: Hypothalamus, temperature regulation, and feeding in the rat. Am. J. Physiol. Leg. Content **221**(3), 800–807 (1971)
27. Zhao, Z.D., Yang, W.Z., Gao, C.C., Fu, X., Zhang, W., Zhou, Q., Chen, W.P., Ni, X.Y., Lin, J.K., Yang, J.: A hypothalamic circuit that controls body temperature. Proc. Natl. Acad. Sci. **114**(8), 2042–2047 (2017)
28. Wang, Y.Y., Qin, J., Han, Y., Cai, J., Xing, G.G.: Hyperthermia induces epileptiform discharges in cultured rat cortical neurons. Brain Res. **1417**(15), 87–102 (2011)
29. Simon, H.B.: Hyperthermia. N. Engl. J. Med. **329**(7), 483 (1993)
30. Erecinska, M., Thoresen, M., Silver, I.A.: Effects of hypothermia on energy metabolism in Mammalian central nervous system. J. Cereb. Blood Flow Metab. **23**(5), 513–530 (2003)
31. Orlowski, J.P., Erenberg, G., Lueders, H., Cruse, R.P.: Hypothermia and barbiturate coma for refractory status epilepticus. Crit. Care Med. **12**(4), 367–372 (1984)
32. Arendt, T., Stieler, J., Holzer, M.: Brain hypometabolism triggers PHF-like phosphorylation of tau, a major hallmark of Alzheimer's disease pathology. J. Neural Transm. (Vienna) **122**(4), 531–539 (2015)
33. Kim, J., Connors, B.: High temperatures alter physiological properties of pyramidal cells and inhibitory interneurons in hippocampus. Front. Cell. Neurosci. **6**(10), 27 (2012)
34. Ye, M.Y., Yang, J., Tian, C.P., Zhu, Q.Y., Yin, L.P., Jiang, S., Yang, M.P., Shu, Y.S.: Differential roles of NaV 1.2 and NaV 1.6 in regulating neuronal excitability at febrile

temperature and distinct contributions to febrile seizures. Sci. Rep. **8**(1), 753 (2018)
35. Yu, Y.G., Hill, A.P., Mccormick, D.A.: Warm body temperature facilitates energy efficient cortical action potentials. PLoS Comput. Biol. **8**(4), e1002456 (2012)
36. Thompson, S.M., Masukawa, L.M., Prince, D.A.: Temperature dependence of intrinsic membrane properties and synaptic potentials in hippocampal CA1 neurons in vitro. J. Neurosci. **5**(3), 817–824 (1985)
37. Volgushev, M., Kudryashov, I., Chistiakova, M., Mukovski, M., Niesmann, J., Eysel, U.T.: Probability of transmitter release at neocortical synapses at different temperatures. J. Neurophysiol. **92**(1), 212–220 (2004)
38. Dinkelacker, V., Voets, T., Neher, E., Moser, T.: The readily releasable pool of vesicles in chromaffin cells is replenished in a temperature-dependent manner and transiently overfills at 37 C. J. Neurosci. **20**(22), 8377–8383 (2000)
39. Hardingham, N.R., Larkman, A.U.: The reliability of excitatory synaptic transmission in slices of rat visual cortex in vitro is temperature dependent. J. Physiol. **507**(1), 249–256 (1998)
40. Yu, Y.G., Shu, Y.S., McCormick, D.A.: Cortical action potential backpropagation explains spike threshold variability and rapid-onset kinetics. J. Neurosci. **28**(29), 7260–7272 (2008)
41. McCormick, D.A., Huguenard, J.R.: A model of the electrophysiological properties of thalamocortical relay neurons. J. Neurophysiol. **68**(4), 1384–1400 (1992)
42. Strong, S.P., Koberle, R., Steveninck, R.R.D.R.V., Bialek, W.: Entropy and information in neural spike trains. Phys. Rev. Lett. **80**(1), 197–200 (1996)
43. Haider, B., Duque, A., Hasenstaub, A.R., Mccormick, D.A.: Neocortical network activity in vivo is generated through a dynamic balance of excitation and inhibition. J. Neurosci. **26**(17), 4535 (2006)
44. Isaacson, J.S., Scanziani, M.: How inhibition shapes cortical activity. Neuron **72**(2), 231–243 (2011)
45. Priebe, N.J., Ferster, D.: Direction selectivity of excitation and inhibition in simple cells of the cat primary visual cortex. Neuron **45**(1), 133–145 (2005)
46. Bennett, C., Arroyo, S., Hestrin, S.: Subthreshold mechanisms underlying state-dependent modulation of visual responses. Neuron **80**(2), 350–357 (2013)
47. Wang, L.F., Jia, F., Liu, X.Z., Song, Y., Yu, L.C.: Temperature effects on information capacity and energy efficiency of Hodgkin–Huxley neuron. Chin. Phys. Lett. **32**(10), 108701 (2015)
48. Gewaltig, M.O., Diesmann, M., Aertsen, A.: Propagation of cortical synfire activity: survival probability in single trials and stability in the mean. Neural Netw. **14**(6–7), 657–673 (2001)
49. Reyes, A.D.: Synchrony-dependent propagation of firing rate in iteratively constructed networks in vitro. Nat. Neurosci. **6**(6), 593–599 (2003)
50. Haider, B., Häusser, M., Carandini, M.: Inhibition dominates sensory responses in the awake cortex. Nature **493**(7430), 97 (2013)
51. Mittmann, W., Koch, U., Häusser, M.: Feed-forward inhibition shapes the spike output of cerebellar Purkinje cells. J. Physiol. **563**(2), 369–378 (2005)
52. Higley, M.J., Contreras, D.: Balanced excitation and inhibition determine spike timing during frequency adaptation. J. Neurosci. **26**(2), 448–457 (2006)
53. Schreiber, S., Fellous, J.-M., Tiesinga, P., Sejnowski, T.J.: Influence of ionic conductances on spike timing reliability of cortical neurons for suprathreshold rhythmic inputs. J. Neurophysiol. **91**(1), 194–205 (2004)
54. Dube, C.M., Brewster, A.L., Baram, T.Z.: Febrile seizures: mechanisms and relationship to epilepsy. Brain Dev. **31**(5), 366–371 (2009)

Publisher's Note Springer Nature remains neutral with regard to jurisdictional claims in published maps and institutional affiliations.